Proc. Natl. Acad. Sci. USA
Vol. 88, pp. 10895–10899, December 1991
Biochemistry

Crystals of a ternary complex of human immunodeficiency virus type 1 reverse transcriptase with a monoclonal antibody Fab fragment and double-stranded DNA diffract x-rays to 3.5-Å resolution

(antibody cocrystallization/DNA cocrystallization/AIDS/polymerase structure/protein–nucleic acid interaction)

ALFREDO JACOBO-MOLINA†, ARTHUR D. CLARK, JR.†, ROGER L. WILLIAMS†, RAYMOND G. NANNI†, PATRICK CLARK‡, ANDREA L. FERRIS§, STEPHEN H. HUGHES§, AND EDWARD ARNOLD†

†Center for Advanced Biotechnology and Medicine and Rutgers University Chemistry Department, 679 Hoes Lane, Piscataway, NJ 08854-5638; ‡Program Resources, Inc.; and §Advanced BioScience Laboratories–Basic Research Program, National Cancer Institute–Frederick Cancer Research and Development Center, P.O. Box B, Frederick, MD 21702-1201

Communicated by Aaron J. Shatkin, September 12, 1991 (received for review July 15, 1991)

ABSTRACT **Two crystal forms of complexes have been grown that contain human immunodeficiency virus type 1 reverse transcriptase and a monoclonal antibody Fab fragment. One of the crystal forms (form II, space group $P3_112$, $a = 168.7$ Å, $c = 220.3$ Å) diffracts x-rays to 3.5-Å resolution and appears suitable for moderate-resolution structure determination. The form II crystals have the unusual property that their maximum resolution of diffraction and resistance to radiation damage are enhanced by either crystallization in the presence of or soaking with double-stranded DNA primer–template mimics. These crystals may permit structural studies of catalytically relevant complexes and eventually enable us to experimentally observe successive steps in the reverse transcription process.**

AIDS, caused by the human immunodeficiency virus (HIV), is a fatal disease with no known cure. HIV reverse transcriptase (RT) is the target of the most widely used treatments for AIDS. Because RT is a polymerase, many of its inhibitors are nucleoside analogs, such as 3′-azido-3′-deoxythymidine (AZT) and dideoxynucleosides (e.g., dideoxyinosine and dideoxycytosine), that, when incorporated into the growing DNA chain, result in chain termination (reviewed in ref. 1). However, some of the most potent and selective inhibitors of HIV-1 RT—for example, the recently reported diazepinone derivatives (2, 3)—are not nucleoside analogs and may inhibit by a different mechanism.

HIV-1 RT isolated from virions consists of a heterodimer containing two polypeptide chains of 66 and 51 kDa (p66 and p51) (4). The two polypeptides have the same amino-terminal sequences. The p51 chain is produced by the cleavage of either the HIV-1 RT p66 or a larger precursor by the HIV-1 protease. When the p66 form of HIV-1 RT is expressed in *Escherichia coli* (5), a "bacterially processed" p66/p51 heterodimer can be prepared that has termini and catalytic properties similar to those of the enzyme found in virions. This heterodimer was used for the present work.

It is anticipated that a three-dimensional structure of HIV-1 RT will accelerate the development of more effective agents for the treatment of AIDS. As methods for structure-based refinement of pharmaceutical agents improve, knowledge of the HIV-1 RT structure will become increasingly valuable. The structure of HIV-1 RT could be used both to search for new drugs and to guide the efficient improvement of existing inhibitors. There are problems with even the most successful of the available inhibitors of HIV-1 RT; for example, drug-resistant viral mutants arise rapidly in patients treated with AZT (6). A combination of inhibitors with varied targets on HIV-1 (7) is more likely to provide a successful treatment for AIDS than is any single agent.

Many laboratories have made extensive efforts to produce crystals of HIV-1 RT that are suitable for x-ray analysis (e.g., refs. 8–12). There are no published reports of crystals that diffract to a resolution sufficient for a complete atomic description of the enzyme. We have used a variety of approaches to "engineer crystallizability," including protein engineering aimed at changing the specific amino acids on the surface, making complexes with antibody fragments, or making complexes with synthetic nucleic acids that mimic primer–template substrates. In this paper, we describe conditions that allowed us to obtain crystals of HIV-1 RT p66/p51 heterodimer complexed with the antigen-binding fragment (Fab fragment) of a monoclonal antibody that diffract x-rays to 4-Å resolution. We also demonstrate that these crystals can accommodate double-stranded DNA (dsDNA) molecules of defined sequence. In the presence of nucleic acid, the resolution of the diffraction pattern increases to 3.5 Å.

MATERIALS AND METHODS

Purification of HIV-1 RT p66/p51 Heterodimer. During the purification of HIV-1 RT p66/p66 homodimer from a bacterial expression system (13), Q-Sepharose fractions containing p66/p51 heterodimer were diafiltered into 20 mM Tris (pH 8.0) and then loaded onto an HR 10/10 Mono Q anion-exchange column (Pharmacia) previously equilibrated with 50 mM diethanolamine (pH 8.9). The column was developed with a linear gradient from 0 to 240 mM NaCl in the same buffer at 4 ml/min. The peak material at 180 mM NaCl corresponding to p66/p51 heterodimer was finally loaded onto two Sephadex G-75 superfine columns (2.5 × 90 cm; Pharmacia) connected in series and was eluted with 20 mM Tris, pH 8.0/100 mM NaCl at 0.25 ml/min. Purified p66/p51 heterodimer was either used immediately or stored at −80°C.

Purification of mAb28 and Production and Purification of Fab28. The relative affinities of nine monoclonal antibodies (mAbs) for the HIV-1 RT p66/p51 heterodimer were determined (data not shown). The mAb designated mAb28 (14),

The publication costs of this article were defrayed in part by page charge payment. This article must therefore be hereby marked "*advertisement*" in accordance with 18 U.S.C. §1734 solely to indicate this fact.

Abbreviations: HIV-1, human immunodeficiency virus type 1; RT, reverse transcriptase; mAb, monoclonal antibody; Fab, antigen-binding fragment; CHESS, Cornell High Energy Synchrotron Source; dsDNA, double-stranded DNA; SAS, saturated ammonium sulfate.

Table 1. Crystallization conditions for HIV-1 RT p66/p51 complexes

Complex	Total protein conc., mg/ml	Crystallization solution	Maximum dimensions, mm	Time for growth, days
RT–Fab28 (form I)	7	50 mM Tris, pH 8.0/38% SAS	0.2 × 0.2 × 0.25	7–28
RT–Fab28 (form II)	15	100 mM cacodylate, pH 5.6/34% SAS	0.4 × 0.6 × 1.2	4
RT–Fab28–DNA	12	100 mM cacodylate, pH 5.6/30% SAS	0.4 × 0.4 × 1.0	4–7

Crystallization was carried out in hanging-drop vapor diffusion experiments at 4°C with starting drop volumes of 4–8 μl suspended over reservoirs containing 1 ml of the crystallization solution. The hanging drops were prepared by adding equal volumes of the crystallization and the concentrated protein solutions, and the resulting initial protein concentration is listed. In the cocrystallization experiments that included dsDNA oligomers, 1 μl of a solution containing annealed oligomers at 1 nmol/μl in 10 mM Tris, pH 7.5/100 mM NaCl/0.5 mM EDTA was added to 7-μl hanging drops to give a 2-fold molar excess of DNA.

which had the highest affinity for the enzyme, was selected for cocrystallization with RT. Ascites fluid containing mAb28 was diluted 5-fold with 1.5 M glycine, pH 8.9/3 M NaCl and loaded at a flow rate of 5 ml/min onto a previously equilibrated 25-ml protein A-Sepharose column (Pharmacia). After extensive washing, the bound mAb was eluted with 100 mM sodium citrate (pH 3.0) into a tube containing 1 M Tris (pH 8.8). Purified mAb28 was diafiltered into 50 mM sodium acetate (pH 5.5) and stored at −80°C.

Purified mAb28 was treated with papain crosslinked to agarose beads (Sigma) with shaking for 8 hr at 34°C. The resulting digest was filtered through a 0.22-μm Millex filter unit and then loaded onto an HR 10/10 Mono S cation-exchange column (Pharmacia) equilibrated with 50 mM sodium acetate (pH 5.5). The flowthrough fraction containing Fab28 was diafiltered into 20 mM Tris, pH 8.0/25 mM NaCl and loaded onto an HR 10/10 Mono Q column equilibrated with 20 mM Tris (pH 8.0) and was eluted using a linear gradient from 75 to 85 mM NaCl in the same buffer. The major isoelectric form was collected and either used immediately for crystallization experiments or stored at −80°C.

Preparation of Oligodeoxynucleotides. Oligonucleotides were synthesized in an Applied Biosystems DNA synthesizer (model 380B) using 1-μmol-scale columns. Three oligonucleotides (and their complements) were prepared:

```
15-mer:      5′-CGCCCGAACAGGGAC-3′
17-mer:    5′-GGCGCCCGAACAGGGAC-3′
19-mer: 5′-ATGGCGCCCGAACAGGGAC-3′
```

After purification by anion-exchange chromatography, complementary DNA strands were annealed in 10 mM Tris, pH 7.5/100 mM NaCl/0.5 mM EDTA by standard heating/cooling protocols.

Complex Formation and Analysis. The appropriate mixing ratio of HIV-1 RT p66/p51 and Fab28 for complex formation was estimated using polyacrylamide gel electrophoresis under nondenaturing conditions. A 1 mg/ml solution of each protein was prepared using a Centricon-10 microconcentrator (Amicon). The Fab was mixed in a range of ratios with a constant amount of the p66/p51 heterodimer. These mixtures were run in a PhastSystem native PAGE (Pharmacia). The empirically determined mass ratio required for stoichiometric complex formation was 1 RT to 0.82 Fab. Complexes of RT–Fab28 were also analyzed and purified on a Mono Q column; however, a fraction of the complex dissociated during chromatography, reducing the utility of this approach.

Crystallization and Crystal Treatment. Two different crystal forms containing HIV-1 RT p66/p51 heterodimer and Fab28 have been obtained (Table 1). Purified RT and Fab28 were concentrated separately in Centricon-30 and Centricon-10 microconcentrators (Amicon), respectively, concomitantly exchanging the buffer with 10 mM Tris, pH 8.0/75 mM NaCl, and then were mixed at a mass ratio of 1 RT to 0.82 Fab to give a final concentration of 14 mg/ml (form I) or 30 mg/ml (form II). The form II crystals have also been grown in the presence of dsDNA oligomers (Table 1).

Form I crystals of RT–Fab28 grew from precipitates when a mixture of isoelectric variants of Fab28 was used. When these crystals were grown using a single isoelectric variant of Fab28, they reached full size within 1 week. Form II crystals with and without DNA grew rapidly and reproducibly (Fig. 1).

Crystals were mounted into capillaries directly from hanging drops. Crystal soaking with dsDNA oligomers was carried out in hanging drops as follows. Crystals were transferred from the mother liquor to fresh 8-μl hanging drops containing 7 μl of 50% (vol/vol) saturated ammonium sulfate (SAS) in 100 mM cacodylate (pH 5.6) and 1 μl of dsDNA (1 nmol/μl) in 10 mM Tris, pH 7.5/100 mM NaCl/0.5 mM EDTA. Crystals were mounted after a period of several hours or sooner if cracking or other morphological damage became apparent.

Diffraction Experiments. X-ray diffraction data collection was carried out using the rotation method on either a multiwire electronic area-detector system on a rotating anode or photographic film at a synchrotron source. Studies at the Center for Advanced Biotechnology and Medicine/Waksman Biomolecular Crystallography Laboratory utilized a Xuong–Hamlin Mark II area detector (San Diego Multiwire Systems) on a Rigaku RU-200 rotating-anode x-ray generator. Experiments at the Cornell High Energy Synchrotron Source (CHESS) used beamlines A1 (λ = 1.565 Å) and F1 (λ = 0.91 Å) for monochromatic oscillation x-ray exposures and B2 for polychromatic (Laue) x-ray data exposures.

RESULTS AND DISCUSSION

Although a number of laboratories, including our own, have described crystals of HIV-1 RT p66/p51 heterodimer, none of those crystals were of sufficient quality for complete structure determination (reviewed in ref. 12). Cocrystallization of HIV-1 RT with an antibody Fab fragment may facilitate structure determination. (*i*) When the Fab fragments are bound to RT,

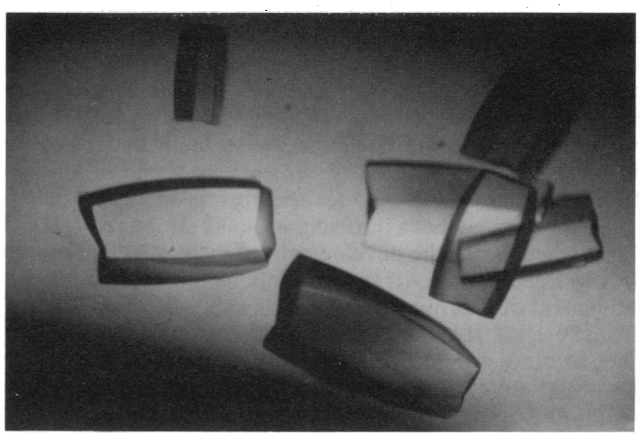

FIG. 1. Form II crystals of HIV-1 RT complexed with Fab28. Conditions for growth are given in Table 1. The maximum dimensions of crystals pictured here are 0.7 × 0.4 × 0.3 mm.

Table 2. Highest resolution of x-ray diffraction recorded from crystals of complexes of HIV-1 RT with Fab28 and dsDNA oligomers

Complex	Resolution, Å		
	Area detector (1.54 Å)	Synchrotron	
		1.56 Å	0.91 Å
RT–Fab28 (form I)	>50	25*	6
RT–Fab28 (form II)	7.5	4.5	4.0
Form II cocrystallized with dsDNA	6.6	3.7	3.5
Form II soaked with dsDNA	—	3.5	3.5

Area-detector data collection was performed using a Xuong–Hamlin Mark II area-detector system (San Diego Multiwire Systems) in the Center for Advanced Biotechnology and Medicine/Waksman Biomolecular Crystallography Laboratory. Synchrotron data collection was performed using x-ray film at CHESS on the A1 (λ = 1.56 Å) and F1 (λ = 0.91 Å) beamlines. Every entry in the table corresponds to the result of experiments with at least two crystals. In the case of the synchrotron experiments with the form II crystals, each resolution entry corresponds to experiments using at least five separate crystals. All resolution entries refer to measurements made during data collection using the rotation method and correspond to data with $\langle I/\sigma(I)\rangle$ at least 2.0. For area-detector data collection, 0.1° frames were collected for 60 sec, with the rotating anode-generator operating with a 0.3-mm focal spot at a power between 4 and 5.3 kW. Most oscillation photographs at CHESS covered a range between 0.6° and 2.0° and were exposed between 20 and 60 sec.

*These experiments were carried out when the CHESS A1 station intensity was 3–5 times lower than for the others reported here.

new contacts that could lead to higher-quality crystals are possible and regions involved in undesirable patterns of aggregation may be concealed. (*ii*) Because it is possible that a major barrier to the formation of high-quality crystals of HIV-1 RT is the inherent flexibility of the enzyme, an Fab could serve as a large molecular "clamp" to restrict the conformational freedom of the RT during crystallization. (*iii*) A wealth of structural information is available for Fab fragments, and their structural frameworks are relatively well conserved.

A variety of complexes of protein antigens with antibody Fab fragments have been crystallized and their structures solved (reviewed in ref. 15). For the most part, the protein antigens have been found to have structures that are very similar to the uncomplexed form, although small changes have been detected. Laver *et al.* (16) reported the first crystals of an Fab complex with a protein that had not been previously crystallized, the hemagglutinin-neuraminidase protein of Sendai virus. Prongay *et al.* (17) reported the crystallization of a recombinant version of the HIV-1 gag CA p24 protein in a complex with an antibody Fab fragment. HIV-1 p24 has resisted all other attempts to form crystals, which may be due to a tendency of the protein to spontaneously aggregate to form capsid-like assemblies.

Diffraction Characteristics of the HIV-1 RT–Fab28 Form I Cocrystals. The HIV-1 RT p66/p51–Fab complex form I crystals (12) diffracted x-rays to 6-Å resolution using the CHESS F1 beamline (λ = 0.91 Å) (Table 2). Crystals of a similar size gave poorer diffraction using either the CHESS A1 station (λ = 1.565 Å) or an area detector/rotating anode combination (λ = 1.54 Å). The crystals used for both sets of experiments at CHESS grew in the same crystallization droplet; thus the difference in diffraction is not likely to be due to variations in the inherent crystal properties. The most likely explanation for the dramatic improvement in results with the F1 beamline is the increase in radiation stability of the RT–Fab complex crystals at shorter wavelengths.

Diffraction Characteristics of the HIV-1 RT–Fab28 Form II Cocrystals. The HIV-1 RT–Fab28 complex form II crystals grow as long blocks that often have threefold axial characteristics (Fig. 1). Data have been measured from the form II crystals on an area detector and at CHESS using the F1 and A1 beamlines (Table 2). The description of the unit cell geometry and contents is given in Table 3. The form II crystals have a number of characteristics that are suitable for structure determination. They are reasonably resistant to radiation damage, allowing collection of multiple successive exposures at a single position using synchrotron radiation at CHESS, or collection of a low-resolution (7 Å) data set (with $\langle I/\sigma(I)\rangle$ = 10) from a single crystal by using a rotating anode with an area detector. Crystal mosaicity is relatively low (≈0.2°), as evidenced from polychromatic (Laue) data collection at the CHESS B2 beamline, processing of synchrotron oscillation films, and examination of reflection profiles measured on an area detector.

Improved Diffraction Properties of HIV-1 RT–Fab28 Form II Crystals Containing dsDNA. The most catalytically relevant complexes of HIV-1 RT will include substrates that resemble those in the active reverse transcription complex. RT can copy from RNA or DNA templates. For synthetic convenience and stability we have used dsDNA oligomers for the present studies. The sequences of the oligomers were based on the sequence of the viral genome where the $tRNA_{III}^{Lys}$ primer binds. This is the position where reverse transcription is initiated in HIV-1-infected cells. Lengths were chosen based both on molecular modeling analysis to correspond to the expected length of double-stranded nucleic acid that might be accommodated by the Klenow fragment of *E. coli* DNA polymerase I (19) and on the 18-base-pair (bp) complementarity with $tRNA_{III}^{Lys}$ at the HIV-1 primer-binding site. It has been recently reported that the separation of the polymerase and RNase H active sites of HIV-1 RT corresponds to approximately 15 or 16 nucleotides (20).

A number of the HIV-1 RT–Fab form II crystals were grown in the presence of a 2-fold molar excess of the 19-bp dsDNA fragments. The external morphology and size of these crystals were similar to those of the form II crystals grown in the

Table 3. Unit cell description for HIV-1 RT p66/p51–Fab28 form II crystals with and without DNA

	Space group*	Cell dimensions, Å		No. of complexes per unit cell	Asymmetric unit size		V_M, Å³/Da	Solvent content,‡ %
		a	*c*		Volume, Å³	Mass,† kDa		
RT–Fab28	$P3_112$ (or $P3_212$)	168.7	220.3	12	9.097×10^5	324	2.81	56%
RT–Fab28–DNA§	$P3_112$ (or $P3_212$)	168.9	220.4	12	9.075×10^5	344	2.64	53%

*The Laue symmetry of the form II crystals was determined by comparing intensities for symmetry-related reflections assuming the various possible trigonal and hexagonal point symmetries. Area-detector data sets measured from single crystals that are nearly complete to 7.5-Å resolution have been used for the comparison. The analysis suggested that the Laue symmetry is $P\bar{3}1m$ (R_{merge} = 0.043) and not $P\bar{3}$ (R_{merge} = 0.043) or $P\bar{3}m1$ (R_{merge} = 0.130). The pattern of systematic extinctions for reflections of type 000*l* (*l* = 3*n* for observed reflections) indicates the presence of a 3_1 or 3_2 screw axis along *c*.

†Density of the non-DNA-containing crystals was measured to be 1.16 g/cm³ (18). This is consistent with the asymmetric unit containing two complexes each with one HIV-1 RT p66/p51 heterodimer, one Fab28, and one dsDNA oligonucleotide (when present).

‡Calculated by assuming a standard partial specific volume of 0.74 ml/g for the protein and for the DNA.

§The data given in this entry correspond to a form II RT–Fab28 crystal that had been soaked with a solution containing the 15-bp dsDNA.

absence of DNA. X-ray diffraction experiments were carried out using form II crystals with and without DNA (Table 2). An x-ray diffraction photograph recorded from one of the form II–dsDNA (19 bp) cocrystals is shown in Fig. 2*B*. When compared with a photograph measured from a crystal of similar size of the form II crystals without DNA (Fig. 2*A*), using comparable conditions for oscillation range and exposure, the maximum diffraction resolution improved from 4.0 Å for native crystals to 3.5 Å for DNA-containing crystals. Diffuse scattering that can be seen in diffraction patterns obtained from form II native crystals (Fig. 2*A*) is reduced in form II crystals containing DNA (Fig. 2*B*). In addition, the DNA-containing crystals consistently showed greater resistance to radiation damage than the form II crystals without DNA, extending the usable diffraction lifetime by a factor of ≈2. All of the expected components, HIV-1 RT p66/p51 heterodimer, Fab28, and 19-bp dsDNA oligomers, are present in the crystals both before and after extensive rinsing (Fig. 3).

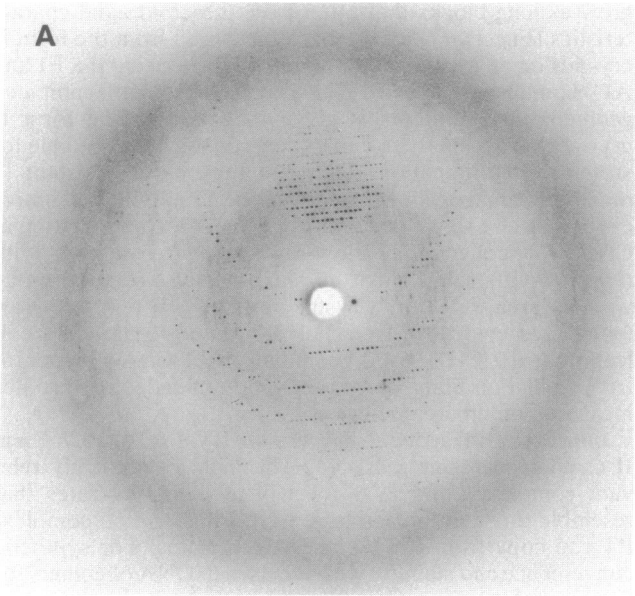

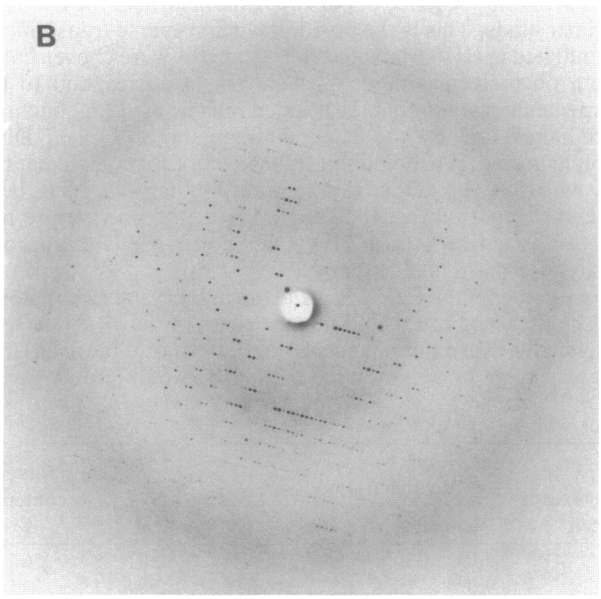

FIG. 2. Diffraction patterns from form II crystals without (*A*) and with (*B*) DNA. Both photographs were measured at the CHESS F1 station (λ = 0.91 Å) with an exposure time of 1 min, oscillation range of 0.6°, and crystal-to-film distance of 188 mm. The size of the crystals used in the two experiments was similar (approximately 0.6 × 0.4 × 0.2 mm). The crystal used for obtaining the photograph in *B* contained a 19-bp dsDNA oligomer. Note the greater diffraction resolution in *B* (3.5 Å) vs. *A* (4.0 Å), as well as a decrease in the amount of diffuse scattering.

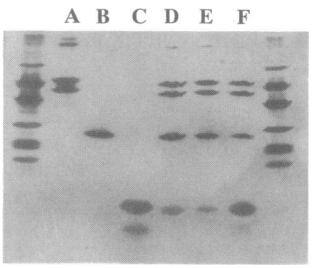

FIG. 3. SDS/PAGE showing presence of all components in the crystals of a ternary complex of HIV-1 RT p66/p51 heterodimer, Fab28, and dsDNA. The gel was run under reducing conditions in an 8–25% polyacrylamide linear gradient and stained with silver (PhastSystem, Pharmacia). Two crystals of comparable size were rinsed in 100 μl of 50% saturated ammonium sulfate in 100 mM cacodylate (pH 5.6) either once (lane D) or 10 times (lane E). The crystals were then dissolved in Laemmli loading buffer (21) and heated for 3 min at 100°C prior to loading. Lanes A, B, and C contained p66/p51, Fab28, and 19-bp dsDNA, respectively. Lane F contained crystallization mother liquor. The two outer lanes contained molecular weight markers with masses 97.4, 66.2, 45.0, 31.0, 21.5, and 14.4 kDa (Bio-Rad). All of the expected components—p66, p51, p25 (antibody Fab chains), and DNA oligomers—are present in the crystals, even after extensive rinsing.

Soaking treatments were tested for their effect on the diffraction properties of the form II crystals. dsDNA oligomers of 15, 17, or 19 bp were added to hanging drops containing form II crystals. A clear improvement of diffraction resolution was observed for a number of these crystals. Many crystals that were soaked for 4 hr in a solution containing a 15-bp dsDNA showed diffraction to 3.5-Å resolution, whereas many similar crystals not containing DNA showed a maximum diffraction resolution of 4.0 Å. The improvement in resolution appeared to be dependent on the specific dsDNA that was used. For example, no apparent improvement in diffraction characteristics was observed for form II crystals cocrystallized with or soaked with a 17-bp dsDNA. In addition, diffraction experiments were carried out using form II crystals soaked with an alternative polyanionic polymer, heparin (Sigma; average M_r = 3500), to control for the specificity of the DNA effect on the crystals. Heparin did not improve the diffraction quality of form II RT–Fab crystals.

Summary of Form II X-Ray Diffraction Data Collection and Crystal Packing. A number of complete data sets have been collected for form II crystals both with and without dsDNA. A representative data set measured from a form II crystal on the area detector shows an R_{merge}¶ of 0.066 for 17,660 observations of 5196 reflections and is 79.6% complete to 6.6-Å resolution. Twelve consecutive oscillation photographs covering a total range of 14° measured from a form II crystal without DNA on the CHESS F1 beamline show an R_{merge} of 0.108 for 3956 observations of 3197 reflections measured to 5.0-Å resolution. A data set measured using the CHESS F1 beamline from form II crystals without DNA is complete to ≈4.5-Å resolution with 3-fold redundancy of measurement for individual reflections.

¶The definition of R_{merge} for both the area detector and film processing is

$$R_{merge} = \Sigma_h [\Sigma_i(I_{hi} - \langle I_h \rangle)/\langle I_h \rangle],$$

where I_{hi} corresponds to the ith observation of an intensity for reflection of index h whose average intensity is $\langle I_h \rangle$.

The unit cell dimensions for form II crystals with and without DNA are quite similar (Table 3). The cell dimensions for crystals determined using both area-detector data and synchrotron film processing and post-refinement (form II native, heavy-atom derivatives, complexes with dsDNA) suggest that the structures with and without DNA are roughly isomorphous. Within eight area-detector data sets, there is a maximum variation of 1 Å in the lengths of *a* and *b* and 0.6 Å in *c*. Comparison of structure-factor amplitudes for data sets from DNA- and non-DNA-containing crystals indicates a change of 20% in the 25- to 8-Å resolution range, vs. errors of 5–8% upon merging data from crystals of the same type. This magnitude of change is consistent with the presence of substantially ordered DNA. It may be possible to obtain an initial low-resolution set of phases by the isomorphous replacement method using the dsDNA addition as a "super-heavy atom."

The 12 complexes in the unit cell of the form II crystals are in a pseudohexagonal arrangement, as evidenced by low-resolution mirror symmetry perpendicular to c^*. The self-rotation function of the form II crystals shows the highest non-origin peak at a value corresponding to a twofold rotation between the two complexes in the crystallographic asymmetric unit along the direction expected from the pseudohexagonal arrangement. Averaging of noncrystallographically equivalent copies of the RT polymerase domains and Fab28 combined with solvent flattening may facilitate phase determination and extension to high resolution (22).

Implications for Future Studies and Possible Model for Structural Disorder of HIV-1 RT. Some of the difficulties in obtaining high-resolution crystals of HIV-1 RT may be due to the inherent properties of the enzyme. For example, HIV-1 RT may require a great deal of conformational flexibility to be able to processively polymerize a DNA strand from either an RNA or a DNA template. Since attempts to crystallize HIV-1 RT itself produced crystals with a low degree of order, it is possible that the surface of the enzyme is well ordered but that the molecule may be relatively flexible in regions that are most intimately involved in enzymatic activity. Another barrier to the formation of high-quality crystals of HIV-1 RT may be aggregation of the protein, particularly in the case of the p66/p66 homodimer. Aggregation of the p66/p66 homodimer may be due in part to the presence of a partially or fully unfolded RNase H domain (12, 23).

The improved diffraction by the form II HIV-1 RT–Fab crystals in the presence of DNA may signify that part of the structural disorder is due to flexibility of the regions of the heterodimer that are in contact with nucleic acid substrates during polymerization. This concept is consistent with the existence of many crystal forms of HIV-1 RT, since the outer surface of the enzyme could still be well organized and participate in long-range lattice contacts. In addition to improved diffraction resolution, there is a significant reduction in the amount of diffuse scattering observed from the form II crystals when DNA is present. This result is also indicative of improved order in the form II crystals containing DNA, since diffuse scattering often connotes the presence of disordered fiber-like structures. The remarkable result that either cocrystallization or soaking with dsDNA oligomers improves the diffraction pattern suggests that these crystals may have special relevance for catalytic studies.

Note Added in Proof. In recent experiments at CHESS we have observed diffraction from the RT–Fab28–DNA form II crystals at 3.1-Å resolution. We have also obtained a low-resolution structure of HIV-1 RT based on an electron density map computed using five heavy-atom derivative data sets at 7-Å resolution.

We are very grateful to all members of both of our laboratories for their dedicated contributions to this work. We thank Amnon Hizi for cloning HIV-1 RT; Gail Ferstandig Arnold, Helen Berman, and Aaron Shatkin for critical reading of the manuscript; Aaron Shatkin and Marvin Cassman for support of and interest in this work; Xiaode Lu for special help in a number of areas; Dave Miller for growing cells; Anqiang Zhang, Thomas Li, Deena Oren, Dawn Rubenstein, Allen Smith, and Charles Zahner for help in synchrotron data collection; Don Bilderback and the entire CHESS staff for their excellent help in support of the X-ray diffraction studies; and Dick Leidich for assistance in the area-detector studies. E.A. gratefully acknowledges the following for financial support of this work: National Institutes of Health Grants AI26790 and GM39558, the New Jersey Commission on Science and Technology, and Johnson & Johnson through James Gaylor for a postdoctoral fellowship (to A.J.-M.). E.A. is an Alfred P. Sloan Foundation Research Fellow. The research in the laboratory of S.H.H. was sponsored in part by the National Cancer Institute under Contract NO1-CO-74101 with Advanced BioScience Laboratories and the National Institute of General Medical Sciences, and NO1-CO-74102 with Program Resources, Inc./DynCorp.

1. Mitsuya, H., Yarchoan, R. & Broder, S. (1990) *Science* **249**, 1533–1544.
2. Pauwels, R., Andries, K., Desmyter, J., Schols, D., Kukla, M. J., Breslin, H. J., Raeymaeckers, A., Van Gelder, J., Woestenborghs, R., Heykants, J., Schellekens, K., Janssen, M. A. C., De Clercq, E. & Janssen, P. A. J. (1990) *Nature (London)* **343**, 470–474.
3. Merluzzi, V. J., Hargrave, K. D., Labadia, M., Grozinger, K., Skoog, M., Wu, J. C., Shih, C.-K., Eckner, K., Hattox, S., Adams, J., Rosenthal, A. S., Faanes, R., Eckner, R. J., Koup, R. A. & Sullivan, J. L. (1990) *Science* **250**, 1411–1413.
4. Veronese, F. D., Copeland, T. D., DeVico, A. L., Rahman, R., Oroszlan, S., Gallo, R. C. & Sarngadharan, M. G. (1986) *Science* **231**, 1289–1291.
5. Hizi, A., McGill, C. & Hughes, S. H. (1988) *Proc. Natl. Acad. Sci. USA* **85**, 1218–1222.
6. Larder, B. A. & Kemp, S. D. (1989) *Science* **246**, 1155–1158.
7. Arnold, E. & Arnold, G. F. (1991) *Adv. Virus Res.* **39**, 1–87.
8. Lowe, D. M., Aitken, A., Bradley, C., Darby, G. K., Larder, B. A., Powell, K. L., Purifoy, D. J. M., Tisdale, M. & Stammers, D. K. (1988) *Biochemistry* **27**, 8884–8889.
9. Stammers, D. K., Powell, K. L., Larder, B. A., Darby, G., Purifoy, D. J. M., Tisdale, M., Lowe, D. M., Stuart, D. I., Jones, E. Y., Taylor, G. L., Garman, E. F., Griest, R. & Phillips, D. C. (1990) in *Use of X-ray Crystallography in the Design of Antiviral Agents*, eds. Laver, W. G. & Air, G. (Academic, San Diego), pp. 309–319.
10. Unge, T., Ahola, H., Bhikhabhai, R., Backbro, K., Lovgren, S., Fenyo, E. M., Honigman, A., Panet, A., Gronowitz, J. S. & Strandberg, B. (1990) *AIDS Res. Hum. Retroviruses* **6**, 1297–1303.
11. Lloyd, L. F., Brick, P., Mei-Zhen, L., Chayen, N. E. & Blow, D. M. (1991) *J. Mol. Biol.* **217**, 19–22.
12. Jacobo-Molina, A. & Arnold, E. (1991) *Biochemistry* **30**, 6351–6361.
13. Clark, P. K., Ferris, A. L., Miller, D. A., Hizi, A., Kim, K.-W., Deringer-Boyer, S. M., Mellini, M. L., Clark, A. D., Jr., Arnold, G. F., Lebherz, W. B., III, Arnold, E., Muschik, G. M. & Hughes, S. H. (1990) *AIDS Res. Hum. Retroviruses* **6**, 753–764.
14. Ferris, A. L., Hizi, A., Showalter, S. D., Pichuantes, S., Babe, L., Craik, C. S. & Hughes, S. H. (1990) *Virology* **175**, 456–464.
15. Davies, D. R. & Padlan, E. A. (1990) *Annu. Rev. Biochem.* **59**, 439–473.
16. Laver, W. G., Thompson, S. D., Murti, K. G. & Portner, A. (1989) *Virology* **171**, 291–293.
17. Prongay, A. J., Smith, T. J., Rossmann, M. G., Ehrlich, L. S., Carter, C. A. & McClure, J. (1990) *Proc. Natl. Acad. Sci. USA* **87**, 9980–9984.
18. Westbrook, E. M. (1985) *Methods Enzymol.* **114**, 187–196.
19. Ollis, D. L., Brick, P., Hamlin, R., Xuong, N. G. & Steitz, T. A. (1985) *Nature (London)* **313**, 762–766.
20. Furfine, E. S. & Reardon, J. E. (1991) *J. Biol. Chem.* **266**, 406–412.
21. Laemmli, U. (1970) *Nature (London)* **227**, 680–685.
22. Arnold, E. & Rossmann, M. G. (1986) *Proc. Natl. Acad. Sci. USA* **83**, 5489–5493.
23. Davies, J. F., Hostomska, Z., Hostomsky, Z., Jordan, S. R. & Matthews, D. A. (1991) *Science* **252**, 88–95.